PNAS RESEARCH ARTICLE | GENETICS

Sexual stage–specific A-to-I mRNA editing is mediated by tRNA-editing enzymes in fungi

Zhuyun Bian[a], Zeyi Wang[a], Diwen Wang[a], and Jin-Rong Xu[a,1]

Edited by N. Louise Glass, University of California, Berkeley, CA; received November 2, 2023; accepted February 20, 2024

A-to-I RNA editing catalyzed by adenosine-deaminase-acting-on-RNA (ADARs) was assumed to be unique to metazoans because fungi and plants lack ADAR homologs. However, genome-wide messenger RNA (mRNA) editing was found to occur specifically during sexual reproduction in filamentous ascomycetes. Because systematic characterization of adenosine/cytosine deaminase genes has implicated the involvement of *TAD2* and *TAD3* orthologs in A-to-I editing, in this study, we used genetic and biochemical approaches to characterize the role of *FgTAD2*, an essential adenosine-deaminase-acting-on-tRNA (ADAT) gene, in mRNA editing in *Fusarium graminearum*. *FgTAD2* had a sexual-stage-specific isoform and formed heterodimers with enzymatically inactive *FgTAD3*. Using a repeat-induced point (RIP) mutation approach, we identified 17 mutations in *FgTAD2* that affected mRNA editing during sexual reproduction but had no effect on transfer RNA (tRNA) editing and vegetative growth. The functional importance of the H352Y and Q375*(nonsense) mutations in sexual reproduction and mRNA editing were confirmed by introducing specific point mutations into the endogenous *FgTAD2* allele in the wild type. An in vitro assay was developed to show that FgTad2-His proteins purified from perithecia, but not from vegetative hyphae, had mRNA editing activities. Moreover, the H352Y mutation affected the enzymatic activity of FgTad2 to edit mRNA but had no effect on its ADAT activity. We also identified proteins co-purified with FgTad2-His by mass spectrometry analysis and found that two of them have the RNA recognition motif. Taken together, genetic and biochemical data from this study demonstrated that FgTad2, an ADAT, catalyzes A-to-I mRNA editing with the stage-specific isoform and cofactors during sexual reproduction in fungi.

ascosporogenesis | A-to-I editing | sexual reproduction | *Fusarium graminearum* | *Gibberella zeae*

A-to-I editing catalyzed by adenosine deaminases acting on RNA (ADAR) enzymes can alter the hereditary information of mRNA in metazoans (1). Despite the absence of ADAR orthologs, genome-wide A-to-I RNA editing was found to specifically occur during sexual reproduction in *Fusarium graminearum* (2), which is a major causal agent of Fusarium Head Blight (FHB) of wheat and barley (3). *F. graminearum* is a haploid, homothallic ascomycete that produces sexual fruiting bodies known as perithecia. Four-celled ascospores (sexual spores) are physically discharged from perithecia and become airborne to infect flowering wheat or barley heads (4, 5). Because ascospores are the primary inoculum of FHB, sexual reproduction plays a critical role in the infection cycle of *F. graminearum* (3). Among the 70 genes with premature stop codons (PSC) in their coding region that require A-to-I editing to encode full-length functional proteins, several of them have been functionally characterized, including the *PUK1*, *FgAMA1, FgBUD14,* and *AMD1* genes that play important roles in ascospore development (2, 6–8). Whereas the *Fgama1* mutant forms single-celled round ascospores that may grow by budding within asci, the *Fgbud4* and *Fgamd1* mutants are defective in crozier formation and ascus development, respectively.

Stage-specific A-to-I RNA editing also specifically occurs during sexual reproduction in other Sordariomycetes, including *Neurospora crassa*, *Neurospora tetrasperma*, *Fusarium verticillioides*, *Sordaria macrospora*, and *Pyronema confluens* (9–11). All these fungi, in fact all the fungi that have been sequenced, have no genes that encode proteins with both adenosine deaminase and dsRNA binding domains, which are the hallmarks of ADARs. Although the average editing level is similar between *F. graminearum* and metazoans, they differ in the distribution of editing sites. In *F. graminearum*, the majority of editing sites (over 70%) are in the coding region and result in codon changes (2). In humans, 99.6% of editing sites are in non-coding regions and do not affect protein coding (11). Furthermore, in *F. graminearum* and other fungi, A-to-I editing has a strong preference of U at the −1 position and tends to occur in the loops of predicted mRNA structures (11, 12). In humans and other metazoans, editing occurs preferentially in the stem (dsRNA) regions of mRNA and has no distinct preference for U at the −1 position (11). These observations strongly suggest that RNA editing in fungi involves an editing machinery independent of ADARs.

Significance

Genome-wide A-to-I mRNA editing occurs specifically during sexual reproduction in filamentous fungi that lack ADARs. In this study, we used genetic and biochemical approaches to characterize the *FgTAD2* gene that encodes an adenosine deaminase acting on tRNA (ADAT) and showed that it is responsible for catalyzing A-to-I RNA editing in the wheat head blight fungus *Fusarium graminearum*. *FgTAD2* is well conserved in fungi as an essential gene required for tRNA editing during vegetative growth, but it has a sexual stage–specific isoform in *F. graminearum* and the model filamentous fungus *Neurospora crassa*. Our data indicate that ADAT enzymes homologous to FgTad2 are responsible for A-to-I mRNA editing during sexual reproduction, possibly involving sexual stage-specific isoforms and co-factors.

Author affiliations: [a]Department of Botany and Plant Pathology, Purdue University, West Lafayette, IN 47907

Author contributions: Z.B. and J.-R.X. designed research; Z.B., Z.W., and D.W. performed research; Z.B., Z.W., and J.-R.X. analyzed data; and Z.B. and J.-R.X. wrote the paper.

The authors declare no competing interest.

This article is a PNAS Direct Submission.

[1]To whom correspondence may be addressed. Email: jinrong@purdue.edu.

This article contains supporting information online at https://www.pnas.org/lookup/suppl/doi:10.1073/pnas.2319235121/-/DCSupplemental.

Published March 11, 2024.

The *F. graminearum* genome has 18 genes that are predicted to encode proteins with adenosine or cytosine deaminase (ACD) domains. Targeted deletion mutants were generated by gene replacement for all but two of these 18 *ACD* genes (13). However, none of the 16 *ACD* deletion mutants had specific defects in RNA editing. Deletion of the other two *ACD* genes that are orthologous to yeast *TAD2* and *TAD3* appears to be lethal in *F. graminearum*. In the budding yeast *Saccharomyces cerevisiae*, *TAD2* and *TAD3* are two essential genes encoding adenosine deaminase acting on tRNA (ADAT) proteins that are responsible for the editing of A^{33} in the anticodon of tRNA (14). The Tad3 protein is likely enzymatically inactive due to the E to V mutation in the catalytic core of the adenosine deaminase domain, but it is essential to form heterodimers with Tad2 for editing of tRNAs (14). *TAD1*, the other ADAT gene in yeast, is dispensable for growth and tRNA editing. In *F. graminearum*, the *FgTAD1* deletion mutant also has no detectable phenotype and no defect in RNA editing (2). Thus, *FgTAD2* and *FgTAD3* are the only two adenosine deaminase domain–containing genes in *F. graminearum* that could not be ruled out for their roles in A-to-I editing. In *Escherichia coli*, the TadA ADAT protein alone can catalyze A-to-I mRNA editing although at a relatively low efficiency (15). Because FgTad3, similar to yeast Tad3, has the E to V mutation in the deaminase domain, FgTad2 may act alone or it may interact with FgTad3 together with other stage-specific cofactors to catalyze mRNA editing in *F. graminearum*.

To determine the RNA editing mechanism in fungi, we characterized the functions of *FgTAD2* in A-to-I mRNA editing in *F. graminearum* in this study. Repeat induced point mutation (RIP) that introduces C to T mutations into repetitive sequences (16–18) was used to generate ascospore progeny with random mutations in *FgTAD2*. Among 17 RIP mutations identified in nine ascospore progeny with defects in ascosporogenesis but normal in growth, two of them, H352Y mutation and nonsense mutation at Q375 (Q375*), were identified in more than one of the RIP progeny. Both the H352Y and Q375* mutations were verified to affect the function of *FgTAD2* in ascosporogenesis and mRNA editing. Furthermore, the editing of *PUK1* transcripts with affinity-purified FgTad2 proteins from perithecia was detected in an in vitro assay developed in this study. Under the same reaction conditions, FgTad2 proteins purified from vegetative hyphae or perithecia of the $FgTAD2^{352Y}$-His mutant retained ADAT activities but could not edit in vitro transcripts of *PUK1*. Mass spectrometry analysis identified dozens of FgTad2-interacting proteins (FIPs), including two proteins with RNA recognition motifs (RRMs). Overall, results from our genetic and biochemical studies demonstrated that FgTad2, an ADAT, is responsible for A-to-I mRNA editing during sexual reproduction in *F. graminearum*.

Results

Identification of Short Transcripts of *FgTAD2* during Sexual Reproduction. Based on published RNA-seq data, *FgTAD2* had two major transcript isoforms. Whereas the longer transcripts contain the full-length predicted ORF, the shorter ones have the entire deaminase domain and two upstream in-frame ATG codons, M113 and M181 (Fig. 1*A*). Interestingly, *FgTAD2*-L transcripts are constitutively expressed, but *FgTAD2*-S transcripts are expressed specifically during sexual reproduction and account for over 60% of *FgTAD2* transcripts (Fig. 1*B*). The FgTad2 orthologs are well conserved in other filamentous fungi. In *N. crassa*, *NcTAD2* also had two transcript isoforms, and *NcTAD2*-S was the specific and dominant isoform during sexual reproduction (Fig. 1*C*). Similar observations of two transcripts of the *TAD2* ortholog were observed in *F. verticillioides*, another fungus reported to have A-to-I mRNA editing (Fig. 1*C*).

To test whether M113 (A^{337}TG) and M181 (A^{541}TG) act as start codons for *FgTAD2*-S, we introduced the T to G mutation at T^{338} and T^{542} of *FgTAD2*. The resulting $FgTAD2^{M113R}$ and $FgTAD2^{M181R}$ mutant alleles were then transformed into the wild-type strain PH-1 to replace the endogenous *FgTAD2* gene (*SI Appendix*, Fig. S1). Three $FgTAD2^{M113R}$ and three $FgTAD2^{M181R}$ transformants (*SI Appendix*, Table S1) were identified and confirmed by PCR and sequencing analysis. All of those transformants were normal in vegetative growth and perithecium formation (Fig. 1*D*). When examined for asci and ascospores, no obvious defects were observed in the $FgTAD2^{M181R}$ transformants. In the $FgTAD2^{M113R}$ transformants, although the majority of asci were aborted, some asci still produced ascospores with various morphological defects (Fig. 1*E*). Therefore, M113 is likely the main start codon for *FgTAD2*-S, but M181 may be used as an inefficient alternative in the $FgTAD2^{M113R}$ transformant for ascospore formation.

Although Tad3 is enzymatically inactive, it interacts with Tad2 to form heterodimers for tRNA editing in the budding yeast *S. cerevisiae* (14). To assay the interaction between FgTad2 and FgTad3, we generated the *FgTAD2*-S and *FgTAD3*-3xFLAG constructs and transformed them into PH-1. In proteins isolated from hyphae of the resulting transformants, FgTad2 was found to co-immunoprecipitate with FgTad3 (Fig. 1*E*), indicating their interaction in vivo, likely forming heterodimers in *F. graminearum*. Interestingly, *FgTAD3* also has two transcript isoforms, with the short transcripts being specifically expressed during sexual reproduction. However, although the *FgTAD3*-S and *FgTAD3*-L transcripts differ in the lengths of their 5′-UTRs, they contain the same open reading frame because the predicted ATG is still in the *FgTAD3*-S transcripts (Fig. 1*F*).

Identification of RIP Mutations in *FgTAD2*. To identify RIP mutations in *FgTAD2*, we transformed a nonfunctional fragment ($FgTAD^{340–*1512}$, Fig. 1*A*) into PH-1. The resulting transformant T2R (*SI Appendix*, Table S1) was normal in growth and perithecium formation but often produced ascospores with abnormal morphologies (Fig. 2*A*). Ascospores released from T2R perithecia at 10 days post-fertilization (dpf) were used for single-spore isolation. Because studies with the *PUK1, FgAMA1, FgBUD14,* and *AMD1* genes have indicated the importance of RNA editing in ascospore formation (2, 6–8), we isolated ascospores with morphological defects (Fig. 2*A*). Among the 497 isolated single ascospores (Fig. 2*B*), 436 had no obvious or only minor defects in growth or sexual reproduction but 52 failed to form colonies, likely due to the occurrence of RIP mutations that are lethal or detrimental to hyphal growth. Only nine ascospore progeny had no or only minor defects in vegetative growth but displayed severe defects in sexual reproduction. All of them produced darkly pigmented perithecia that were smaller (*SI Appendix*, Fig. S2) than those formed by the wild type (Fig. 2*C*) and lacked asci or ascospores (Fig. 2*D*).

We then amplified and sequenced the endogenous *FgTAD2* allele with primers T2Rseq-F and T2Rseq-R (Fig. 1*A*). All nine ascospore progeny contained at least one RIP mutation resulting in amino acid changes in *FgTAD2* (Table 1). A total of 17 non-synonymous RIP mutations was identified and all of them were C to T or G to A mutations. Sixteen of them are between M181 and G381, a region containing the deaminase domain of FgTad2 (Fig. 2*E*). Two of these RIP mutations were identified in more than one ascospore progeny (Table 1). Three progeny, P148, P149, and P438, had the C^{1132}-to-T RIP mutation that results in the change of H352 to tyrosine. Whereas P148 and

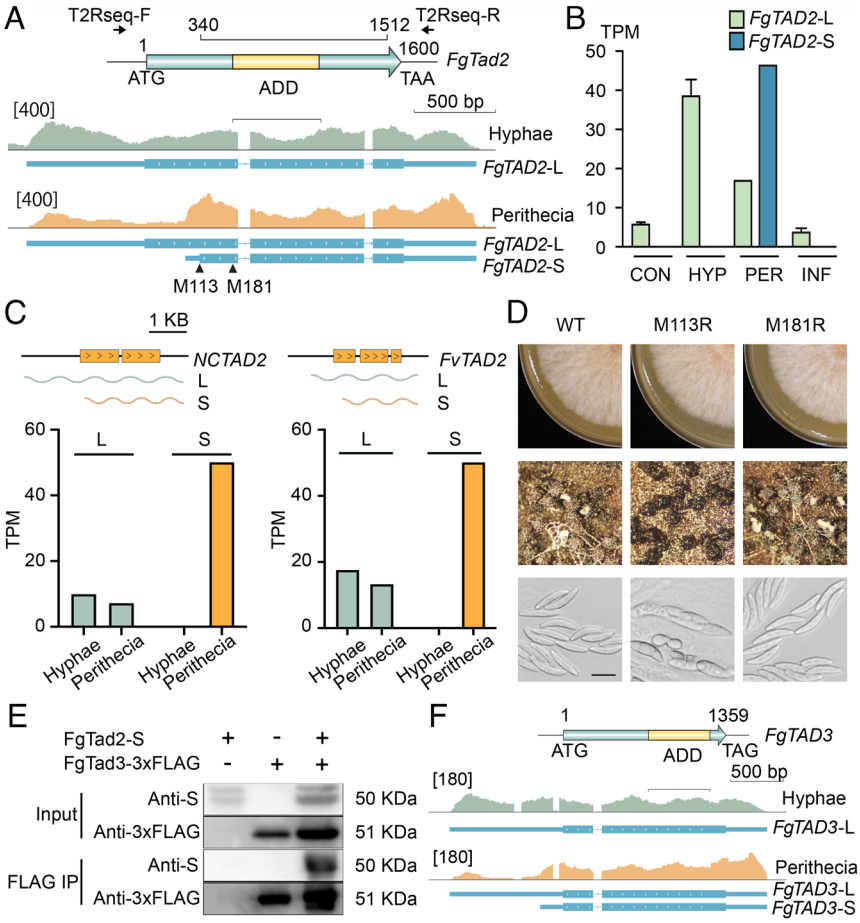

Fig. 1. Two transcript isoforms of *FgTAD2* and their expression profiles. (*A*) Diagrams of the *FgTAD2* gene and IGV-Sashimi plots showing the read coverage and transcript isoforms of *FgTAD2* in RNA-seq data of 24-h hyphae and 8-dpf perithecia. *FgTAD2*-L is constitutively expressed, but *FgTAD2*-S transcripts are present only in perithecia. M113 and M181 are two in-frame start codons upstream from the ADD. TR2seq-F and TR2seq-R, primers for sequencing the endogenous *FgTAD2* allele. ADD, adenosine deaminase domain. 340 to 1512, the fragment of *FgTAD2* integrated ectopically into PH-1. Numbers in brackets on the left indicate the coverage range. The first two introns are in the 5′-UTR. (*B*) The abundance of *FgTAD2*-L and *FgTAD2*-S transcripts in conidia (CON), vegetative hyphae (HYP), 8-dpf perithecia (PER), and infected wheat heads (3-dpi; INF). TPM, transcripts per million. (*C*) Two transcript isoforms of *FvTAD2* and *NcTAD2*. The shorter one was specifically expressed during sexual reproduction. (*D*) Colonies, perithecia, and asci of the wild type and the *FgTAD2*^{M113R} and *FgTAD2*^{M181R} mutants. The *FgTAD2*^{M113R} mutant had defects in ascospore formation and release. (Bar: 20 μm.) (*E*) Western blots of total proteins (input) isolated from transformants expressing the FgTad2-S and FgTad3-3×FLAG constructs and proteins eluted from anti-FLAG beads (FLAG IP) were detected with an anti-S or anti-FLAG antibody. (*F*) Diagrams of the *FgTAD3* gene and IGV-Sashimi plots showing the read coverage and transcript isoforms of *FgTAD3* in RNA-seq data of 24-h hyphae and 8-dpf perithecia. *FgTAD3*-L is constitutively expressed but *FgTAD3*-S transcripts are present only in perithecia.

P149 had additional RIP mutations, P438 had only the H352Y mutation (Table 1). Progeny P195 and P456 both had a nonsense mutation at Q375 (Q375*, Table 1) that results in the truncation of the C-terminal 115 aa region of *FgTAD2*. Whereas P195 had another mutation, P456 had only the Q375* mutation.

Verification of the Effect of the H352Y Mutation in *FgTAD2* on Ascosporogenesis. H352 of FgTad2 is conserved in its orthologs from other filamentous ascomycetes such as *F. verticillium*, *N. crassa,* and *S. macrospora*, but not in Tad2 of *S. cerevisiae* and *S. pombe* that lack A-to-I editing (Fig. 3*A*). To confirm the mutational effect of H352Y, we generated the *FgTAD2*^{H352Y}-*hph* gene replacement construct carrying the C^{1132} to T mutation and transformed it into PH-1 (*SI Appendix*, Fig. S1). Three *FgTAD2*^{H352Y} transformants were identified and confirmed by sequencing analysis to have the endogenous *FgTAD2* replaced by the transforming mutant allele. All of the *FgTAD2*^{H352Y}, transformants were normal in vegetative growth but had severe defects in sexual reproduction (Fig. 3*B*). Similar to progeny P438, *FgTAD2*^{H352Y} transformants formed small, melanized perithecia that lacked asci or ascospores in most of them (Fig. 3*B*). In over 200 perithecia examined carefully, approximately 1.5% of them had a few elongated asci containing abnormal ascospores at 14 dpf (*SI Appendix*, Fig. S3). These results confirmed the detrimental effects of the H352Y mutation on ascosporogenesis in *F. graminearum*.

To assay the effect of the H352Y mutation on editing, RNA was isolated from perithecia of the wild type and the *FgTAD2*^{H352Y} transformant and used for RT-PCR amplification and sequencing. Because A-to-I RNA editing was observed originally in the *PUK1* kinase gene that contains two PSCs, UA^{1831}G and UA^{1834}G, in its kinase domain (2), we first sequenced RT-PCR products of *PUK1*. In the wild type, the editing level was greater than 90% at both A^{1831} and A^{1834} (Fig. 3*C*). However, only single peaks representing the unedited A^{1831} and A^{1834} of *PUK1* were detected in the *FgTAD2*^{H352Y} transformant (Fig. 3*C*). We then selected FG2G05470 and FG4G18510 (named as *RTT1* and *RTT2* for RT-PCR target genes below) for verification because they both contain one edited site in the predicted loops with editing levels higher than 60%. In the wild type, the editing level at A^{655} of *RTT1* was approximately 60%. However, editing was not observed at A^{655} in the *FgTAD2*^{H352Y} mutant (Fig. 3*D*). Similarly, over 90% of A^{1358} of *RTT2* was edited in the wild type, but the *FgTAD2*^{H352Y} mutant had no detectable editing event at this position (Fig. 3*D*).

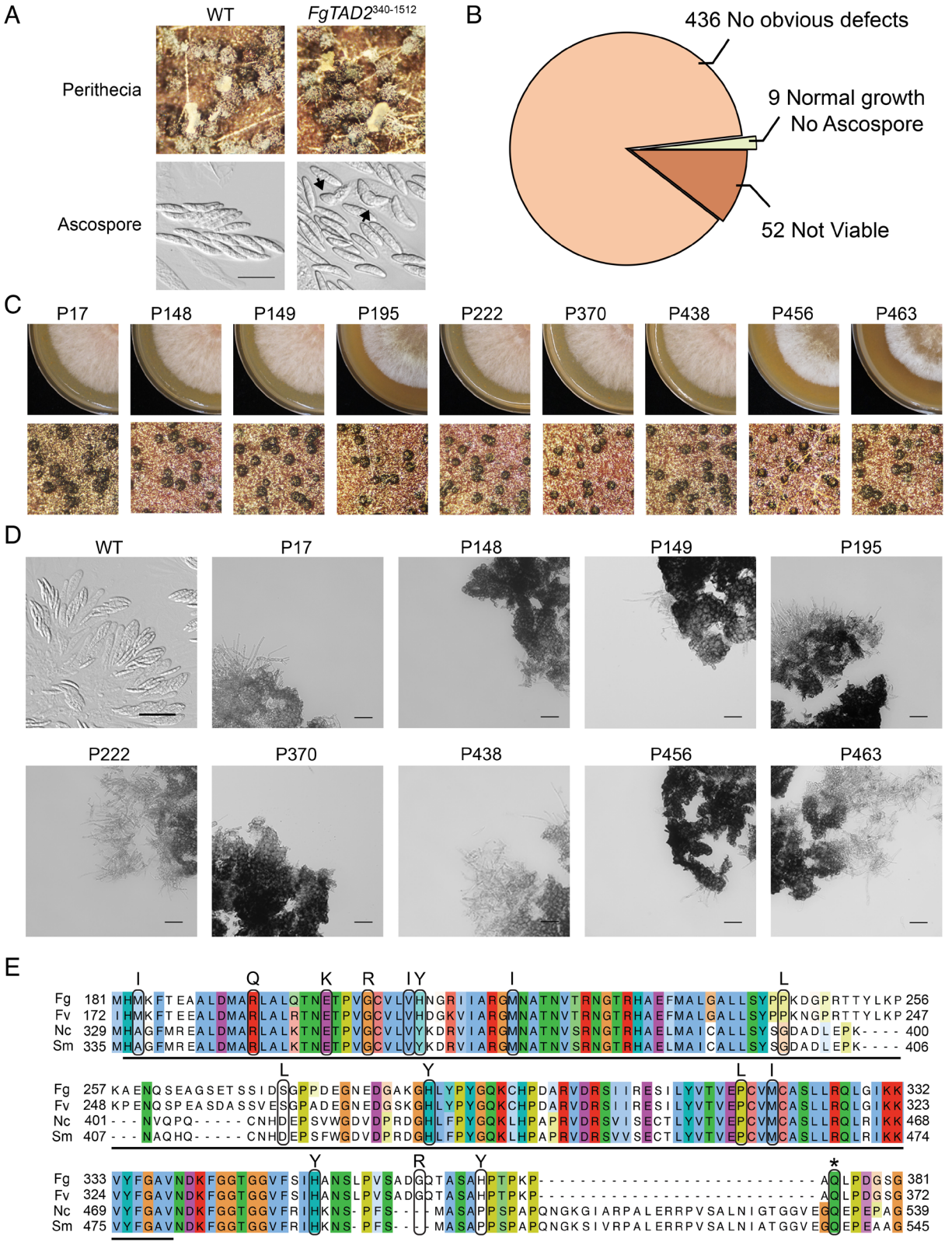

Fig. 2. RIP progeny with mutations in *FgTAD2* affecting ascosporogenesis and RNA editing. (*A*) V8 cultures, perithecia, and ascospores of the wild type and *FgTAD2*$^{340-1512}$ transformant. Ascospores with abnormal morphology were marked with arrows. (Bar: 20 μm.) (*B*) Categorizing 497 ascospores isolated by single spore-isolation for their defects in growth and ascosporogenesis. (*C*) V8 and mating cultures of the wild type and marked RIP progeny. (*D*) Perithecia of the marked strains were examined for the formation of asci and ascospores. (Bar: 40 μm.) (*E*) Alignment of the marked region of FgTad2 and its orthologs from *Fusarium verticillium* (Fv), *Neurospora crassa* (Nc), and *Sordaria macrospora* (Sm). RIP mutations identified in this region are boxed with black lines and marked with amino acid changes on the top. *, stop codon.

To confirm the defect of the *FgTAD2*^{H352Y} mutant in RNA editing, we then conducted RNA-seq analysis with the same RNA samples isolated from 6-dpf perithecia. Whereas over 26,000 editing sites were identified in the wild type, only 1,899 editing sites were detected in the *FgTAD2*^{H352Y} mutant (Fig. 3*E*). The average editing level was less than 6% in the *FgTAD2*^{H352Y} mutant

Table 1. RIP mutations identified in nine ascospore progeny

Progeny	Mutation	Amino acid changes
P17	G703 to A	V209 to I
	G735 to A	M219 to I
P148	C1132 to T	H352 to Y
	C706 to T	H210 to Y
	C1180 to T	H368 to Y
	C1235 to T	S386 to Y
P149	C812 to T	P245 to L
	C896 to T	S273 to L
	C937 to T	H287 to Y
	C1132 to T	H352 to Y
P195	G679 to A	E201 to K
	C1201 to T	Q375 to stop
P222	C1028 to T	P317 to L
P370	G1038 to A	M320 to I
	G1162 to A	G362 to R
P438	C1132 to T	H352 to Y
P456	C1201 to T	Q375 to stop
P463	G549 to A	M183 to I
	G659 to A	R194 to Q
	G691 to A	G205 to R

but over 19% in the wild type (Fig. 3*E*). These results indicate that the H352Y mutation in *FgTAD2* results in a significant reduction in RNA editing in both editing events and editing levels. In these RNA-seq data, editing events at A^{1831} and A^{1834} of *PUK*, A^{655} of *RTT1*, and A^{1358} of *RTT2* were detected in the wild type but not in the *FgTAD2*^{H352Y} mutant (Fig. 3*F*), which is consistent with sequencing analysis of RT-PCR products. For the genes retaining editing levels ≥20% in the *FgTAD2*^{H352Y} mutant, clustering analysis with their expression profiles showed that there is no enrichment for genes highly expressed at earlier sexual developmental stages (*SI Appendix*, Fig. S4).

The Q375* Mutation in *FgTAD2* Affects Ascosporogenesis. To verify the effect of the Q375* mutation identified in progeny P195 and P456, we generated the *FgTAD2*^{Q375*}-*hph* gene replacement construct carrying the $C^{1201}AG$ to $T^{1201}AG$ mutation (*SI Appendix*, Fig. S1) and transformed it into PH-1. Three *FgTAD2*^{Q375*} transformants were identified and confirmed for the replacement of endogenous *FgTAD2* with *FgTAD2*^{Q375*}. They were normal in growth but produced small, melanized perithecia (Fig. 3*B*). No asci or ascospores were observed in over hundreds of perithecia examined at 14 dpf (Fig. 3*C*). These observations confirmed that the nonsense mutation at Q375 is responsible for phenotypes observed in RIP progeny with the Q375* mutation.

To verify the effect of the nonsense mutation at Q375 on RNA editing, we also isolated RNA from perithecia formed by the *FgTAD2*^{Q375*} transformant at 6 dpf. Sequencing analysis with RT-PCR products showed that A-to-I editing was not detected at A1831 and A1834 of *PUK1*, A655 of *RTT1*, and A1358 of *RTT2* (Fig. 3*D*). RNA-seq analysis also showed that both editing events and editing levels (Fig. 3*E*) were significantly reduced in the *FgTAD2*^{Q375*} transformant. Similar to the *FgTAD2*^{H352Y} mutant, the editing events retained in the *FgTAD2*^{Q375*} mutant are not enriched in genes expressed at earlier sexual developmental stages (*SI Appendix*, Fig. S4). Because the nonsense mutation at Q375 results in the truncation of the C-terminal 115 amino acid residues, the C-terminal region of FgTad2 must be dispensable for its ADAT activities during vegetative growth but important for its functions in RNA editing and ascosporogenesis during sexual reproduction. It is possible that this region is necessary for the interaction of FgTad2 with other sexual stage-specific proteins or cofactors that are involved in A-to-I editing.

Editing of In Vitro Transcripts of *PUK1* by FgTad2 Proteins Purified from Perithecia. To purify FgTad2 proteins from *F. graminearum*, we generated the *FgTAD2*-His construct and transformed it into PH-1. Total proteins were isolated from hyphae harvested from 24-h YEPD cultures and perithecia formed by *FgTAD2*-His transformants at 6 dpf. FgTad2-His and its interacting proteins were isolated with Ni-NTA agarose beads (19). Affinity-purified FgTad2 proteins were first assayed for ADAT activities with in vitro transcripts of $tRNA^{Ala}_{AGC}$ as the substrate, in which editing of A^{33} to I creates a *Sty*I site (Fig. 4*A*). After editing reactions, $tRNA^{Ala}_{AGC}$ transcripts were used as the template for RT-PCR, and the resulting PCR products were digested with *Sty*I. As the negative control with no proteins added, only a single 72-bp band was detected. In samples treated with FgTad2-His proteins purified from hyphae or perithecia, digestion with *Sty*I resulted in the detection of the 43-bp and 29-bp bands (Fig. 4*B*). These results indicate that affinity-purified FgTad2 proteins have the expected ADAT activities.

We then used the same reaction conditions to assay A-to-I editing at A^{1831} and A^{1834} in in vitro transcripts of *PUK1*. In samples treated with FgTad2 proteins purified from 24-h hyphae, no editing events were detected by sequencing (Fig. 4*C*). However, in samples treated with FgTad2 proteins purified from 6-dpf perithecia, both A and G (double peaks) could be detected at A^{1831} and A^{1834} in *PUK1* transcripts (Fig. 4*D*), indicating the occurrence of A-to-I editing at these two sites. The editing level was approximately 60% and 55%, respectively, at A^{1831} and A^{1834} of *PUK1* in three independent replicates (Fig. 4*D*). These results indicated that FgTad2 proteins affinity purified from perithecia but not from vegetative hyphae have A-to-I editing activities with the *PUK1* mRNA template.

The H352Y Mutation in FgTad2 Affects Its Editing Activities on mRNA Substrates. To determine its effect on in vitro mRNA editing, we introduced the H352Y mutation into the *FgTAD2*-His construct by overlapping PCR and transformed the resulting *FgTAD2*^{H352Y}-His gene replacement construct into transformant HY2 (*SI Appendix*, Table S1). The resulting transformants were normal in vegetative growth and displayed the same defects in ascosporogenesis as in the *FgTAD2*^{H352Y} mutant (*SI Appendix*, Fig. S5). The expression of FgTad2^{H352Y}-His fusion proteins was confirmed by western blot analysis (*SI Appendix*, Fig. S5). In assays with FgTad2^{H352Y}-His proteins purified from 6-dpf perithecia, editing of A^{33} in the $tRNA^{Ala}_{AGC}$ template was detected (Fig. 5*A*), indicating that the H352Y mutation does not affect the ADAT activity of FgTad2, which is consistent with the normal growth rate of the *FgTAD2*^{H352Y} mutant. We then assayed editing activities of FgTad2^{H352Y} proteins with the *PUK1* mRNA as the substrate under the same conditions. Sequencing analysis showed that no editing events were detected at A^{1831} or A^{1834} (Fig. 5*B*). In repeated tries, editing of A^{1831} or A^{1834} was not observed. These results indicated that the H352Y mutation affects the deaminase activity of FgTad2 with the mRNA but not tRNA substrates.

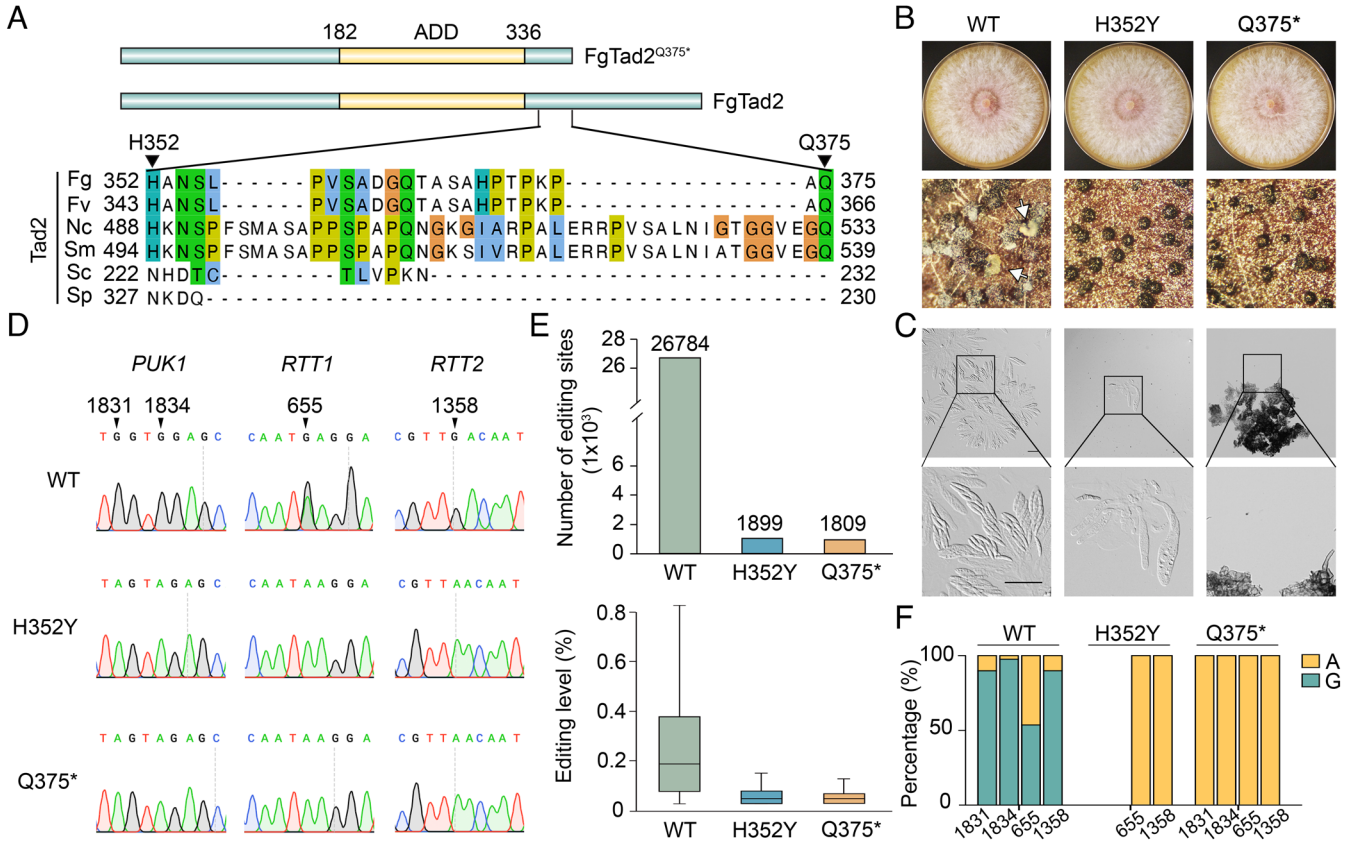

Fig. 3. Verification of the H352Y and Q375* mutations in *FgTAD2* on ascosporogenesis and RNA editing. (*A*) Region of FgTad2 that contains H352 and Q375 and its alignment with orthologs from *Fusarium verticillium* (Fv), *Neurospora crassa* (Nc), *Sordaria macrospora* (Sm), *S. cerevisiae* (Sc), and *Schizosaccharomyces pombe* (Sp). Q375 is marked with a red dot. (*B*) V8 and mating cultures of the wild type and the *FgTAD2*^{H352Y} and *FgTAD2*^{Q375*} mutants. Perithecia formed by the mutants were smaller and lacked ascospore cirrhi (marked with arrows). (*C*) The same set of strains was examined for the formation of asci and ascospores as well as ascogenous hyphae. Perithecia of wild type were examined at 7 dpf. Perithecia of *FgTAD2*^{H352Y} and *FgTAD2*^{Q375*} mutants were examined at 14 dpf. (Bar: 40 μm.) (*D*) Sequencing analysis with RT-PCR products of *PUK1*, *RTT1*, and *RTT2* amplified from mRNA isolated from 6-dpf perithecia of the wild type and the *FgTAD2*^{H352Y} and *FgTAD2*^{Q375*} mutants. Editing of A^{1831} and A^{1834} of *PUK1*, A^{655} of *RTT1*, and A^{1358} of *RTT2* were observed only in the wild type. (*E*) The number of editing sites (*Left*) and editing levels (*Right*) identified by RNA-seq analysis with RNA isolated from perithecia of the indicated strains. (*F*) The percentages of transcripts with A-to-G editing at the marked sites for *PUK1*, *RTT1*, and *RTT2*.

Identification of FgTad2-Interacting Proteins by Affinity Purification. To identify proteins interacting with FgTad2, total proteins isolated from hyphae harvested from 24-h YEPD cultures and 6-dpf perithecia of the FgTAD2-His transformant were co-incubated with Ni-NTA agarose beads. After washing, proteins were eluted from Ni-NTA agarose beads and analyzed by LC MS–MS analysis as described (20). The resulting mass spectrometry data were collected from three biological replicates of both hyphae

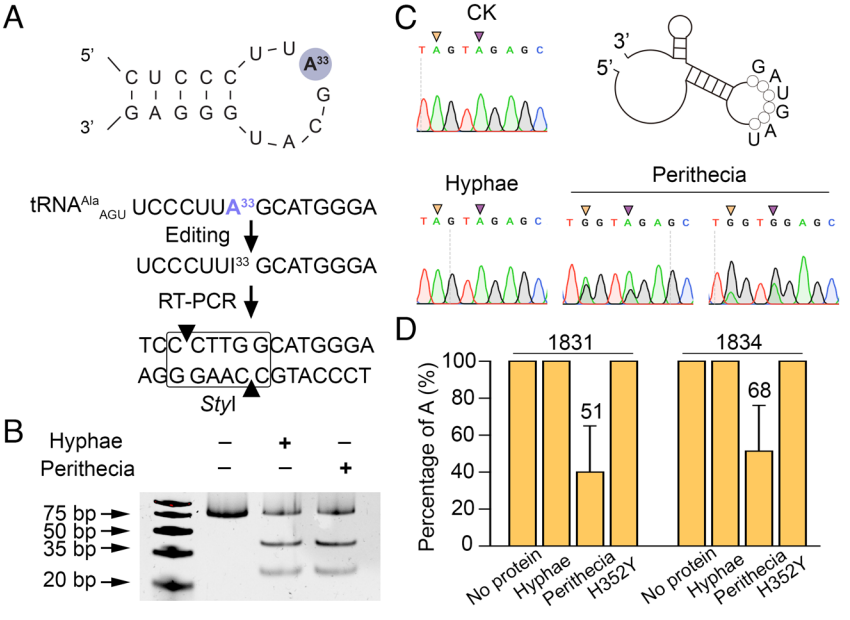

Fig. 4. Editing of in vitro transcripts of *PUK1* by FgTad2 proteins purified from perithecia. (*A*) Diagram of tRNA$^{Ala}_{AGC}$ showing the editing sites and creation of a *StyI* site. (*B*) Assays for tRNA$^{Ala}_{AGC}$ editing at A^{33} by FgTad2 proteins purified from hyphae and perithecia of the *FgTAD2*-His transformants by digestion with *StyI*. CK is the control with no proteins. FgTad2 proteins isolated from either hyphae or perithecia had ADAT activities. (*C*) Sequencing analysis of RT-PCR products amplified from in vitro transcripts of *PUK1* after treatment with FgTad2-His proteins purified from 24-h hyphae or 6-dpf perithecia. Both A^{1831} and A^{1834} of *PUK1* were predicted by RNAfold (https://rna.tbi.univie.ac.at/cgi-bin/RNAWebSuite/RNAfold.cgi) to be on a loop with 20-bp flanking sequences. Double peaks (both A and G) at A^{1831} (yellow arrow) and A^{1834} (purple arrow) were observed only in samples treated with FgTad2 proteins isolated from perithecia. (*D*) Percentage of adenosine at A^{1831} and A^{1834} in *PUK1* mRNA. Mean and SD were estimated with data from three independent replicates.

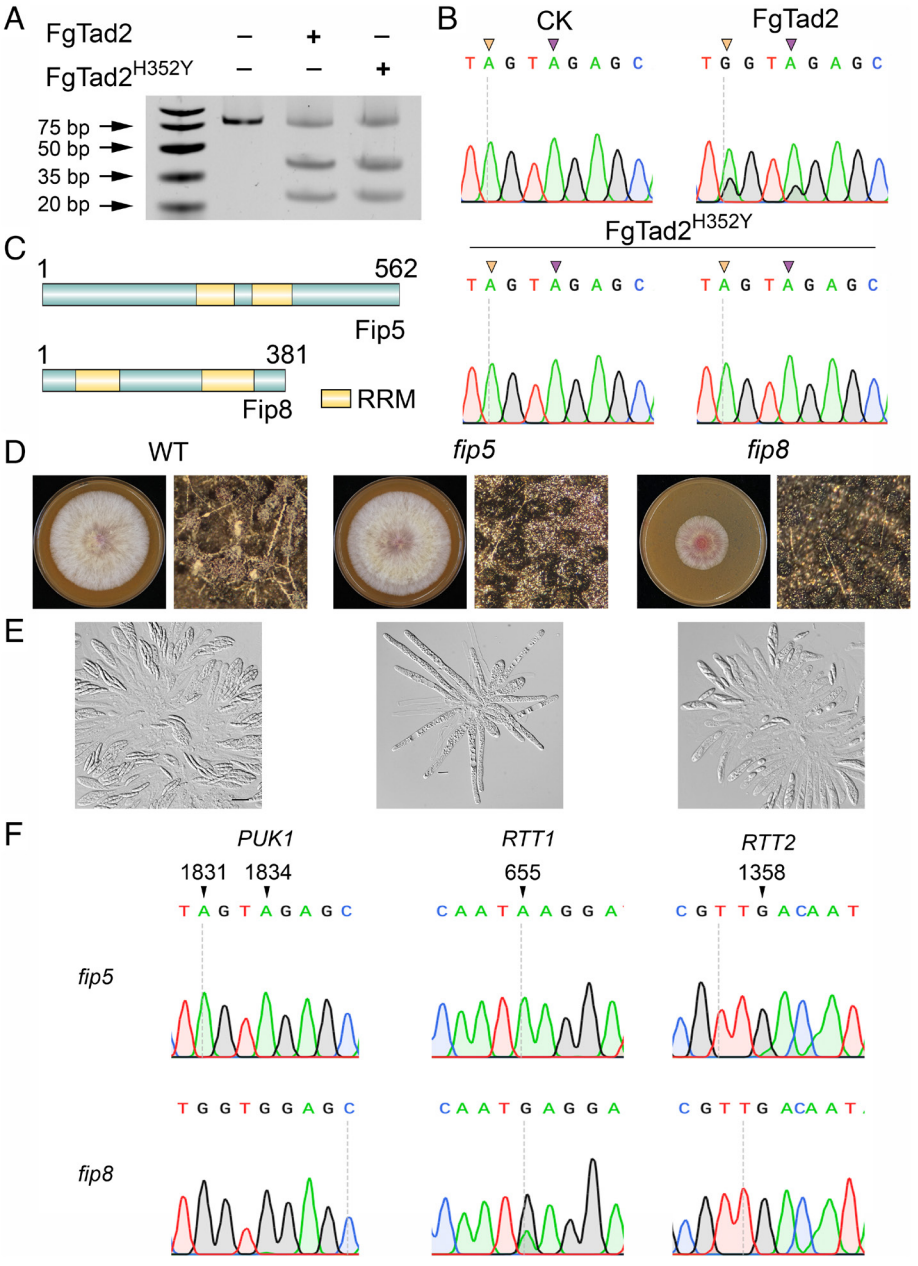

Fig. 5. Defects of FgTad2^{H352Y} proteins in mRNA editing and phenotypes of the *fip5* and *fip8* mutants. (*A*) Assays for tRNA$^{Ala}_{AGC}$ editing at A^{33} by FgTad2 and FgTad2^{H352Y}-his proteins purified from perithecia by digestion with the *Sty*I restriction enzyme. CK is the control with no proteins. FgTad2^{H352Y} proteins had ADAT activities. (*B*) Sequencing analysis of RT-PCR products amplified from in vitro transcripts of *PUK1* after treatment with FgTad2^{H352Y} and FgTad2 proteins purified from 6-dpf perithecia. CK is the control with no proteins. FgTad2^{H352Y} proteins had no mRNA editing activities. (*C*) Diagrams of the Fip5 and Fip8 proteins. RRM, RNA recognition motif. (*D*) Three-day-old V8 cultures of the wild type and *fip5* and *fip8* deletion mutants. Perithecia produced by the *fip5* deletion mutant were smaller than those of the wild type. No ascospore cirrhi were observed in the *fip5* and *fip8* mutants. (*E*) Perithecia formed by the same set of strains were examined for ascus and ascospore formation. (Bar: 20 μm.) (*F*) Sequencing analysis with RT-PCR products of *PUK1*, *RTT1*, and *RTT2* amplified from mRNA isolated from 6-dpf perithecia of the *fip5* and *fip8* mutants. Whereas deletion of *FIP8* had no obvious effect on these editing events, deletion of *FIP5* blocked the editing of A^{1831} and A^{1834} of *PUK1* and A^{655} of *RTT1* but had no significant effect on editing of A^{1358} of *RTT2*.

and perithecia. FgTad3 was identified as a protein interacting with FgTad2 in all three samples of hyphae and perithecia. After filtering out common background proteins, 48 proteins (*SI Appendix*, Table S2) were commonly identified in two or three (2/3 or 3/3) perithecia samples but appeared no more than once (0/3 or 1/3) in hyphal samples. Most of those were specifically expressed or had over twofold upregulation during sexual reproduction based on published RNA-seq data (21). Some of them may function as stage-specific cofactors of FgTad2 for mRNA editing.

Manual annotation identified 17 putative FgTad2-interacting proteins (FIPs) (Table 2) with orthologs in *F. verticillioides* and *N. crassa*. Two of them, *FIP5* and *FIP8*, encode single-stranded DNA (ssDNA)-binding proteins with two RRM domains (Fig. 5*C*). Proteins of RRM domains may enable FgTad2 to interact with mRNA for editing because ADAT proteins, unlike ADARs, lack RNA-binding domains. We then generated the *fip5* and *fip8* deletion mutants (*SI Appendix*, Table S1). Whereas the *fip5* mutant was normal in growth, the *fip8* mutant was reduced in growth rate and aerial hyphal growth (Fig. 5*D*). On mating plates, both the *fip5* and *fip8* mutants formed melanized perithecia. However, perithecia formed by the *fip5* mutant were smaller than those of the wild type (Fig. 5*C*). At 14 dpf, only empty asci with no ascospores were observed in the *fip5* mutant (Fig. 5*E*). In the *fip8* mutant, the majority of asci were aborted and most of the *fip8* asci that produced ascospores contained fewer than eight ascospores (Fig. 5*E*). These results indicate that the *fip5* and *fip8* mutants differ from the *FgTAD2* RIP mutants in defects related to ascus development.

Although the *fip5* mutant formed empty (aborted) asci, it was blocked in ascosporogenesis, which is similar to the *FgTAD2* RIP mutants. We then isolated RNA from perithecia formed by the *fip5* mutant at 6 dpf. Sequencing analysis with RT-PCR products showed that no A-to-I editing could be detected at A1831 and A1834 of *PUK1* and A655 of *RTT1* in the fip5 mutant. However, editing still occurred at A1358 of *RTT2* (Fig. 5*F*), indicating that deletion of *FIP5* affects A-to-I editing at some but not all the editing sites. To our surprise, although the *fip8* mutant had defects

Table 2. FgTad2-interacting proteins identified by affinity purification and MS analysis

Gene name	Gene ID	Annotation
FIP1	FG3G17260	Hypothetical protein
FIP2	FG1G18260	Hypothetical protein
FIP3	FG4G25320	Hypothetical protein
FIP4	FG2G04070	Hypothetical protein
FIP5	FG4G24490	ssDNA-binding protein with RRMs
FIP6	FG3G05040	Hypothetical protein
FIP7	FG3G18580	Hypothetical protein
FIP8	FG4G27920	ssDNA-binding protein with RRMs
FIP9	FG4G36830	Hypothetical protein
FIP10	FG2G24220	Hypothetical protein
FIP11	FG1G41370	Hypothetical protein
FIP12	FG1G50520	Hypothetical protein
FIP13	FG2G16300	Hypothetical protein
FIP14	FG3G28950	Hypothetical protein
FIP15	FG3G01520	Hypothetical protein
FIP16	FG1G40320	Hypothetical protein
FIP17	FG4G25740	Meiosis-specific protein

in ascosporogenesis, editing at all the sites assayed was not significantly affected by deletion of *FIP8* (Fig. 5*F*). These results indicate that *FIP5* may be involved but is not essential for mRNA editing. Editing of mRNA by FgTad2 may involve other stage-specific cofactors during sexual reproduction.

Discussion

Systematic characterization of 18 ACD genes showed that all but two that are orthologous to yeast Tad2 and Tad3 are individually dispensable for A-to-I editing in *F. graminearum*. As in yeast, *FgTAD2* and *FgTAD3* are essential ADAT genes in *F. graminearum* (13). To determine the roles of these two ADAT genes in stage-specific editing of mRNA during sexual reproduction, in this study we used the RIP approach to introduce random mutations into *FgTAD2* by transforming a nonfunctional fragment of *FgTAD2*$^{340–1512}$ (integrated ectopically). Because *FgTAD3* encodes an enzymatically inactive protein that forms heterodimers with FgTad2, it was not pursued in this study. As an essential gene required for tRNA editing, we expect that mutations in *FgTAD2* affecting its ADAT activities will be lethal or detrimental to vegetative growth. Mutations that specifically affect A-to-I mRNA editing during sexual reproduction will have no effect on growth but will cause defects in ascosporogenesis. Indeed, we found that 10.5% of the ascospores isolated by single-spore isolation from the *FgTAD2/FgTAD2*$^{340–1512}$ transformant failed to grow, likely due to RIP mutations affecting tRNA editing. Nevertheless, we identified nine ascospore progeny that had no significant growth defect but were defective in ascosporogenesis. A total of 17 nonsynonymous or nonsense mutations in *FgTAD2* was identified by sequencing analysis with these nine RIP mutants. Two of them, H352Y and Q375*, were identified in more than one of the RIP mutants and further verified for their effects on ascosporogenesis by targeted gene replacement with *FgTAD2* mutant alleles carrying these mutations. These results indicate that mutations in *FgTAD2* affecting sexual reproduction but having no obvious effect on hyphal growth could be successfully isolated by the RIP approach. These RIP mutations may affect the function of FgTad2 in A-to-I mRNA editing and ascosporogenesis but have no effect on tRNA editing and vegetative growth.

The effects of the H352Y and Q375* mutations on A-to-I editing were verified by RNA-seq analysis with RNA isolated from 6-dpf perithecia. In comparison with the wild type, the number of editing events was reduced over 90%, and the average editing level in the *FgTAD2*^{H352Y} and *FgTAD2*^{Q375*} mutants was reduced over 80%. We also sequenced fragments of *PUK1, RTT1,* and *RTT2* amplified by RT-PCR from perithecia and verified that the *FgTAD2*^{H352Y} and *FgTAD2*^{Q375*} mutants had defects in editing of four sites with high editing levels in the wild type (2). The histidine 352 residue is conserved in orthologs of FgTad2 from other Sordariomycetes. Whereas the imidazole ring of histidine allows it to function as a proton donor/acceptor and form a hydrogen bond with other amino acids or nucleic acids to stabilize protein–protein or protein–RNA/DNA complexes, the benzene ring of tyrosine cannot. Therefore, the H353Y mutation may negatively impact the interaction of FgTad2 with its cofactors for binding and editing mRNA. The nonsense mutation at Q375 results in truncation of the C-terminal 115 amino acids. Prediction with AlphaFold2 showed that this C-terminal truncation does not affect the overall catalytic core structure of the FgTad2-FgTad3 heterodimers for tRNA editing, which may explain the normal vegetative growth in the *FgTAD2*^{Q375*} mutant. However, this C-terminal region may be important for FgTad2 to interact with stage-specific cofactor(s) to form complexes with mRNA substrates for binding and editing.

For the other 15 RIP mutations, all of them were identified in only a single RIP mutant. Whereas 14 of them were identified in mutants with two or more RIP mutations in *FgTAD2*, mutant P222 had only the P317L mutation. Although P317 is adjacent to C318, which is one of the four active sites (H231, E233, C318, and C321) in the zinc-binding pocket in FgTad2 based on its alignment with orthologs from other fungi (*SI Appendix*, Fig. S6), RIP mutant P222 had no obvious defects in vegetative growth, indicating that the ADAT activities of FgTad2 are not affected by the P317L mutation. Because of the differences in the size and secondary structures of tRNA and mRNA, it is possible that the P317L mutation may affect the binding and editing of mRNA but have no effect on tRNA editing. Interestingly, the M320I mutation identified in RIP mutant P370 occurs immediately adjacent to C321, which is also involved in the zinc-binding pocket of ADATs (*SI Appendix*, Fig. S6). It may have similar effects with the P317L mutation on mRNA editing. However, mutant P370 had another RIP mutation in *FgTAD2*.

Besides characterizing *FgTAD2* mutant alleles generated by RIP, we also developed an in vitro assay with epitope-tagged FgTad2 proteins purified from *F. graminearum*. As an ortholog of yeast Tad2, an ADAT, it is not surprising that affinity-purified FgTad2 proteins had the ability to edit A^{33} of $tRNA^{Ala}_{AGC}$ in vitro. In editing assays with in vitro transcripts of *PUK1*, we found that only FgTad2-his proteins isolated from perithecia had A-to-I mRNA activity. Under the same conditions, FgTad2-His proteins isolated from vegetative hyphae could edit A^{33} of $tRNA^{Ala}_{AGC}$ but lacked A-to-I mRNA editing activities. These results indicate that FgTad2-His and its interacting proteins isolated by affinity purification from perithecia have mRNA editing activities. Furthermore, we showed that FgTad2 proteins purified from perithecia of the *FgTAD2*^{H352Y}-His mutant retained ADAT activities but failed to edit in vitro transcripts of *PUK1*. Some of these proteins that were co-purified with FgTad2 from perithecia (besides FgTad3) may interact with FgTad2 and function as a stage-specific cofactor(s) enabling FgTad2 ADAT to edit mRNA.

Unlike metazoan ADARs, ADATs lack dsRNA-binding domains, which may be acquired by an ADAT ancestor in ADARs (22). Among the FgTad2-interacting proteins identified by MS analysis, two of them, Fip5 and Fip8, contain RRM domains, and they both specifically associate with FgTad2 in perithecia. The *fip5* and *fip8* mutants also were defective in sexual reproduction, although they differed in phenotype from the *FgTAD2*^{H352Y} and *FgTAD2*^{Q375*} mutants. Whereas the *fip8* mutant produced abnormal ascospores, the *fip5* mutant formed empty asci, likely due to aborted ascospore development. Although it remains possible that *FIP5* and *FIP8* have overlapping functions in interacting with FgTad2 for mRNA editing, other *FIP* genes encoding hypothetical proteins also may be involved. In *E. coli*, the TadA ADAT protein catalyzes A-to-I mRNA editing without the need for interacting with RNA-binding proteins although at a very low frequency. In *E. coli*, only 15 A-to-I RNA editing events were identified (15). In *Xanthomonas oryzae* pv. *oryzicola*, only 30 enriched mRNA targets were identified (23). Furthermore, besides stage-specific cofactor(s), FgTad2 may have stage-specific post-translational modifications that enable the deamination of mRNA substrates during sexual reproduction. Therefore, it is also important to identify and characterize sexual stage–specific post-translational modifications of FgTad2 as well as FgTad3 in *F. graminearum*. It is also worth noting that FgTad3 was present in MS data of all of the hyphal and perithecium samples, but excluded from the list of putative FgTad2-interacting proteins. The stage-specific cofactor(s) of FgTad2 required for mRNA editing may be constitutively expressed but have different isoforms that are similar to the short isoform of FgTad2 (with M113 as the start codon) during sexual reproduction.

Overall, in this study, we used genetic and biochemical approaches to show the importance of *FgTAD2* in A-to-I mRNA editing during sexual reproduction in *F. graminearum*. FgTad2 likely forms heterodimers with FgTad3 and involves stage-specific cofactor(s) or post-translational modifications for mRNA editing in perithecia.

Materials and Methods

Strains and Culture Conditions. The wild-type strain PH-1 (24) and all other strains used in this study were routinely cultured on V8 juice agar plates (20% V8 juice, 0.2% $CaCO_3$, 2% agar) at 25 °C. Growth rate and conidiation in liquid carboxymethyl cellulose (CMC) medium were assayed as described (25). Protoplasts were isolated and used for PEG-mediated transformation as described (25). For selection of transformants, hygromycin B and geneticin (Invitrogen) were added to a final concentration of 300 μg mL^{-1} and 200 μg mL^{-1}, respectively, to the top TB3 agar medium (0.3% yeast extract, 0.3% casamino acids, and 3% glucose). Vegetative hyphae harvested from 24-h liquid YEPD (1% yeast extract, 2% peptone, 2% dextrose) were used for DNA and RNA isolation. Mating and perithecium formation, ascus development, and cirrhus production were assayed on carrot agar plates as described previously (6).

Isolation of RIP Mutants and Identification of RIP Mutations. The *FgTAD2*$^{340–1512}$ fragment was amplified and cloned into *Xho*I-digested plasmid pXY203 by the yeast gap repair approach (26, 27). The resulting *FgTAD2*$^{340–1512}$ construct was transformed into protoplasts of PH-1 (25). Hygromycin-resistant transformants were isolated and confirmed to contain the transforming *FgTAD2*$^{340–1512}$ fragment integrated ectopically. Ascospore cirrhi were collected from perithecia formed by the *FgTAD2*$^{340–1512}$ transformants at 14 dpf and used for single-spore isolation (28). Ascospores with abnormal morphology were isolated and transferred to V8 agar plates for assaying colony growth defects. Ascospore progeny with no obvious growth defects were further assayed for defects in perithecium development and ascospore formation on carrot agar cultures (6). For the nine RIP mutants with severe defects in ascosporogenesis, the endogenous *FgTAD2* allele was amplified with primer pairs T2Rseq-F and T2Rseq-R (Fig. 1*A* and *SI Appendix*, Table S3) and sequenced.

Identification of the Long and Short Isoforms of *FgTAD2* and *FgTAD3*. Based on published RNA-seq data (29), *FgTAD2*-L and *FgTAD2*-S isoforms had the same transcription termination site. Whereas *FgTAD2*-L transcription is initiated at 738 bp upstream from the predicted ATG (M1) in vegetative hyphae, *FgTAD2*-S transcripts with the transcription initiation site at 257 bp downstream from M1 became abundant during sexual reproduction (Fig. 1*A*). With the inputs of these transcription initiation and termination sites, reads mapping to the *FgTAD2*-L and *FgTAD2*-S isoforms were counted and normalized to compute their transcripts per million (TPM) with FeatureCounts (30). The same approach was used to analyze the expression levels of the long and short isoforms of *FgTAD3* as well as the *TAD2* and *TAD3* orthologs in *N. crassa* and *F. verticillioides* by calculating their TPMs with FeatureCounts (30) with published RNA-seq data (9, 29).

Generation of the *FgTAD2*^{M113R}, *FgTAD2*^{M181R}, *FgTAD2*^{H352Y}, and *FgTAD2*^{Q375*} Mutants. To generate the *FgTAD2*^{M113L} allele, full-length *FgTAD2* was amplified by overlapping PCR with primers carrying the AT^{338}G to AG^{338}G mutation (*SI Appendix*, Table S3) and connected to the first 798-bp of hygromycin phosphotransferase (*hph*) cassette amplified from pFL2 (27) by double-joint PCR (31). The upstream flanking sequences of *FgTAD2* were amplified with primers TAD2-1F/T2PM-R and connected to the 5′- end of the *FgTAD2*^{M113R}-*hp* fragment by overlapping PCR. The last 1,187-bp of the *hph* cassette amplified with primers YG/R2HT-R (*SI Appendix*, Table S3) was connected to the *FgTAD2* downstream fragment amplified with primers HTPM-F/TAD2-4R (*SI Appendix*, Table S3) by overlapping PCR. The resulting overlapping PCR products were transformed into protoplasts of PH-1 (25). The resulting *FgTAD2*^{M113R} gene replacement construct was then transformed into protoplasts of PH-1. Hygromycin-resistant transformants with the endogenous *FgTAD2* replaced by the transforming *FgTAD2*^{M113R}-*hph* allele were identified by PCR and confirmed by sequencing analysis. The same approach was used to generate the *FgTAD2*^{M181R} allele with the AT^{542}G to AG^{542}G mutation, the *FgTAD2*^{H352Y} allele with the C^{1132}AT to T^{1132}AT mutation, and the *FgTAD2*^{Q375*} allele with the C^{1123}AG to T^{1123}AG mutation. All the resulting gene replacement constructs with site-specific mutations were transformed into PH-1 to generate mutant strains with the corresponding mutations in *FgTAD2*. For each mutation, at least two independent transformants were identified and confirmed by PCR and sequencing analysis.

Generation of the *FgTAD2*-His and *FgTAD2*^{H352Y}-His Transformants and Affinity Purification of FgTad2 and FgTad2^{H352Y} Proteins. The full-length *FgTAD2* fragment was amplified by PCR with the primer carrying the His-tag sequence (*SI Appendix*, Table S3) and cloned into vector pFL7 by yeast gap repair (27). The *FgTAD2*^{H352Y}-His fusion was generated by introducing the C^{1132}AT to T^{1132}AT mutation in the *FgTAD2*-His vector. The resulting *FgTAD2*-His and *FgTAD2*^{H352Y}-His fusion constructs were confirmed by sequencing and transformed into PH-1. The expression of transforming vectors in transformants expressing *FgTAD2*-His and *FgTAD2*^{H352Y}-His ectopically was analyzed by PCR and western blot analysis (*SI Appendix*, Fig. S5). For affinity purification, total proteins were isolated from 24-h YEPD cultures and perithecia collected from mating plates at 6 dpf as described (32) and incubated with equilibrated Ni-NTA resins (Qiagen) at 4 °C for 1 h with gentle rocking for affinity purification following the manufacturer's instructions. After washing three times, proteins bound to Ni-NTA resins were eluted. The enrichment of FgTad2-His proteins was verified by western blot analysis (*SI Appendix*, Fig. S7) with the anti-His (Thermo-Fisher) antibody.

Preparation of tRNA and mRNA Substrates by In Vitro Transcription. The $tRNA^{Ala}_{AGC}$ cassette containing the T7 RNA polymerase promoter sequence was amplified by PCR primers t65puc19-F (with the *Xba*I sequence) and t65puc19-R (with the *Bsa*I-*Hind*III sequences) (*SI Appendix*, Table S3). The resulting PCR product was digested with *Xba*I and *Hind*III and cloned into pUC19 to generate plasmid pT65. The same approach was used to generate pPUK1 vectors with primer pairs m1puc19-F and m1puc19-R. The pT65 and pPUK1 vectors were linearized with *Bsa*I and used as the template for in vitro transcription with the T7 RNA Polymerase-Plus Enzyme Mix Kit (Invitrogen™) following the instructions provided by the manufacturer. TURBO DNase (1:40 dilution, Invitrogen™) was added to the transcription reaction mixture and incubated for 30 min at 25 °C. After extraction with one volume of acid-phenol:chloroform with IAA (125:24:1, pH 4.5, Invitrogen™) and precipitation with 2.5 volume 100% ethanol, in vitro RNA transcripts were dissolved in refolding buffer (5 mM Tris-HCl, pH 8.0, 150 mM KCl, 1 mM $MgCl_2$) and stored at −80 °C. For secondary structure formation,

tRNA$^{Ala}_{AGC}$ and *PUK1* transcripts were incubated at 70 °C for 5 min and slowly cooled to 25 °C (1 °C per min) as described (33).

In Vitro Deaminase Assays with Affinity-Purified FgTad2 Proteins. The deaminase assay was modified from editing of mRNA by hADA1 and hADAR2 (33). In a reaction volume of 50 μg, in vitro transcripts of tRNA$^{Ala}_{AGC}$ or *PUK1* were mixed with 5 μg of affinity-purified FgTad2 protein in the reaction buffer (50 mM Tris-HCl, pH 8.0, 25 mM KCl, 2.5 mM $MgCl_2$, 1 mM DTT, 0.1 mM EDTA). Protein concentration was assayed with the BCA protein assay kit (Thermo- Fisher) and same amounts of FgTad2-His and FgTad2^{H352Y}-His proteins used in each reaction were verified by western blot analysis. After incubation at 25 °C for 1 h, reactions were stopped by adding 400 μL nuclease-free water and 450 μL of acid-phenol:chloroform. After phenol extraction and precipitation with ethanol, edited tRNA or mRNA substrates were dissolved in 10 μL of nuclease-free water and quantified by measuring absorbance at 260 nm with a NanoDrop DN-1000. For tRNA$^{Ala}_{AGC}$, 1 μg of purified RNA was used as the template for RT-PCR with primers aat65-F and aat65-R (*SI Appendix*, Table S3). To detect editing of A33 on tRNA$^{Ala}_{AGC}$, the resulting PCR products were digested with *Sty*I (New England Biolabs) at 16 °C for 12 h and separated on 12% native polyacrylamide gels (34). For deamination reactions with *PUK1* transcripts, 1 μg of purified RNA was used for RT-PCR with primers aapuk1-F and aapuk1-R. The resulting PCR products were purified with the PCR & DNA Cleanup Kit (New England Biolabs) and sequenced by wide-seq at Purdue Genomic Center. In vitro deaminase assays with affinity-purified FgTad2^{H352Y} were performed under the same conditions as described above. The same amount of FgTad2^{H352Y}-His and FgTad2-His proteins was added to reaction mixtures based on western blot analysis.

RT-PCR and RNA-Seq Analyses. To assay changes in editing, RNA of the wild-type, *FgTAD2*^{H352Y}, and *FgTAD2*Q375* strains was isolated from perithecia collected from mating plates at 6 dpf. For assaying editing sites in *PUK1, RTT1,* and *RTT2*, first-strand cDNA was synthesized with the PrimeScript RT reagent Kit (Takara) and used as the templates for amplification with primers listed in *SI Appendix*, Table S3. The resulting PCR products were purified with the PCR Clean-up kit (New England Biolabs) and sequenced at Eurofin. For RNA-seq analysis, strand-specific RNA-seq libraries were constructed sequenced at the Purdue Genomics Core. RNA-seq reads were aligned to the reference genome of PH-1 using Hisat2 (35). Duplicate reads were eliminated with the MarkDuplicates tool (https://broadinstitute.github.io/picard/) included in the Picard package. After separating sense and antisense strands with the bamtools (36), the resulting read alignments were used to identify A-to-I mRNA editing sites with REDItools as described (37). Reads with editing efficiencies of 20% or higher in the *TAD2*^{H352Y} and *TAD2*^{Q375*} mutants were subsequently mapped to their corresponding genes with TransVar (https://github.com/zwdzwd/transvar). Their expression profiles during sexual development from 1 to 8 dpf were extracted from published RNA-seq data (accession no. PRJNA384311) (6) for clustering analysis with the Mfuzz package.

Identification of FgTad2-Interacting Proteins. To identify FgTad2-interacting proteins, total proteins were isolated from hyphae (24-h YEPD cultures) and 6-dpf perithecia of the *FgTAD2*-His transformant and incubated with Ni-NTA resins (Qiagen) as described above (19). Proteins eluted from Ni-NTA resins were digested with trypsin and further analyzed by nanoflow liquid chromatography–tandem mass spectrometry on a high-resolution hybrid linear ion trap orbitrap mass spectrometer (LTQ-Orbitrap XL; ThermoFisher) coupled to an Agilent Nanoflow LC system. The tandem mass spectrometry data were queried against the National Center for Biotechnology Information nonredundant *F. graminearum* protein database using the SEQUEST algorithm (20) on the Sorcerer IDA server (SageN). We first identified proteins that were present in two or three (2/3 or 3/3) perithecium samples but not more than once (0/3 or 1/3) in hyphal samples and then filtered out proteins encoded by housekeeping genes. Among the 47 putative FgTad2-interacting proteins (*SI Appendix*, Table S2), only 17 of them (Table 2) are intracellular proteins unique to perithecium samples and have orthologs in *N. crassa* and *F. verticillioides* but not in *S. cerevisiae*.

Generation of the *fip5* and *fip8* Mutants. To generate the *FIP5* gene replacement construct by split marker (38), its 650-bp upstream and downstream flanking sequences were amplified using primer pair fip5-7F/ fip5-2R and fip5-3F/ fip5-8R, respectively. Amplified flanking fragments were connected to fragments of the *hph* cassette amplified from vector pFL2 (27) by overlapping PCR using primer pair fip5-1F and fip5-4R. After transforming protoplasts of PH-1 with the resulting PCR products, hygromycin-resistant transformants were isolated and screened for *fip5* mutants by PCR as described (39). The same approach was used to generate the *FIP8* gene replacement constructs and mutants. For each gene, at least two independent deletion mutants were isolated. RNA was isolated from 7-dpf perithecia formed by the *fip5* and *fip8* mutants and analyzed for editing events in *PUK1, RTT1,* and *RTT2* as described above.

Data, Materials, and Software Availability. RNA-seq data of the *FgTAD2*^{H352Y} and *FgTAD2*^{Q375*} transformants have been deposited in NCBI BioProject under the entry number of PRJNA1031222 (40). All other data are included in the article and/or *SI Appendix*.

ACKNOWLEDGMENTS. We thank Dr. Yanyan Wang and Ms. Lilly Shen for assistance with fungal cultures. We also thank Drs. Joseph Flaherty, Cong Jiang, and Huiquan Liu for fruitful discussions and Drs. Larry Dunkle and Steven Goodwin for proofreading. This research was supported by a grant from NSF and a grant from USWBSI to J.-R.X.

1. K. Nishikura, A-to-I editing of coding and non-coding RNAs by *ADARs*. *Nat. Rev. Mol. Cell Biol.* **17**, 83–96 (2016).
2. H. Liu *et al.*, Genome-wide A-to-I RNA editing in fungi independent of *ADAR* enzymes. *Genome Res.* **26**, 499–509 (2016).
3. R. S. Goswami, H. C. Kistler, Heading for disaster: *Fusarium graminearum* on cereal crops. *Mol. Plant Pathol.* **5**, 515–525 (2004).
4. F. Trail, H. Xu, R. Loranger, D. Gadoury, Physiological and environmental aspects of ascospore discharge in *Gibberella zeae* (anamorph *Fusarium graminearum*). *Mycologia* **94**, 181–189 (2002).
5. R. J. Bennett, B. G. Turgeon, Fungal sex: The ascomycota. *Microbiol. Spectrum* **4**, 0005–2016 (2016).
6. S. Cao *et al.*, RNA editing of the *AMD1* gene is important for ascus maturation and ascospore discharge in *Fusarium graminearum*. *Sci. Rep.* **7**, 4617 (2017).
7. C. Hao *et al.*, The meiosis-specific APC activator *FgAMA1* is dispensable for meiosis but important for ascosporogenesis in *Fusarium graminearum*. *Mol. Microbiol.* **111**, 1245–1262 (2019).
8. J. Liang *et al.*, *FgBUD14* is important for ascosporogenesis and involves both stage-specific alternative splicing and RNA editing during sexual reproduction. *Environ. Microbiol.* **23**, 5052–5068 (2021).
9. H. Liu *et al.*, A-to-I RNA editing is developmentally regulated and generally adaptive for sexual reproduction in *Neurospora crassa*. *Proc. Natl. Acad. Sci. U. S. A.* **114**, E7756–E7765 (2017).
10. I. Teichert, T. A. Dahlmann, U. Kuck, M. Nowrousian, RNA editing during sexual development occurs in distantly related filamentous ascomycetes. *Genome Biol. Evol.* **9**, 855–868 (2017).
11. Z. Bian, Y. Ni, J. R. Xu, H. Liu, A-to-I mRNA editing in fungi: Occurrence, function, and evolution. *Cell. Mol. Life Sci.* **76**, 329–340 (2019).
12. C. Feng *et al.*, Uncovering Cis-regulatory elements important for A-to-I RNA editing in *Fusarium graminearum*. *mBio* **13**, e01872-01822 (2022).
13. M. Sun *et al.*, Stage-specific regulation of purine metabolism during infectious growth and sexual reproduction in *Fusarium graminearum*. *New Phytol.* **230**, 757–773 (2021).
14. X. Liu *et al.*, Crystal structure of the yeast heterodimeric *ADAT2/3* deaminase. *BMC Biol.* **18**, 1–14 (2020).
15. D. Bar-Yaacov *et al.*, RNA editing in bacteria recodes multiple proteins and regulates an evolutionarily conserved toxin-antitoxin system. *Genome Res.* **27**, 1696–1703 (2017).
16. M. Freitag, R. L. Williams, G. O. Kothe, E. U. Selker, A cytosine methyltransferase homologue is essential for repeat-induced point mutation in *Neurospora crassa*. *Proc. Natl. Acad. Sci. U.S.A.* **99**, 8802–8807 (2002).
17. E. U. Selker *et al.*, Induction and maintenance of nonsymmetrical DNA methylation in *Neurospora*. *Proc. Natl. Acad. Sci. U.S.A.* **99**, 16485–16490 (2002).
18. L. Guo, L.-J. Ma, "*Fusarium graminearum* genomics and beyond" in *Genomics of Plant-Associated Fungi: Monocot Pathogens* (Springer, 2014), pp. 103–122.
19. A. Spriestersbach, J. Kubicek, F. Schafer, H. Block, B. Maertens, Purification of his-tagged proteins. *Methods Enzymol.* **559**, 1–15 (2015).
20. P. Wang *et al.*, Reciprocal regulation of the TOR kinase and ABA receptor balances plant growth and stress response. *Mol. Cell* **69**, 100–112 (2018).
21. H. Liu *et al.*, Genome-wide A-to-I RNA editing in fungi independent of ADAR enzymes. *Genome Res* **26**, 499–509 (2016).
22. A. P. Gerber, W. Keller, An adenosine deaminase that generates inosine at the wobble position of tRNAs. *Science* **286**, 1146–1149 (1999).
23. W. Nie *et al.*, A-to-I RNA editing in bacteria increases pathogenicity and tolerance to oxidative stress. *PLoS Pathog.* **16**, e1008740 (2020).
24. C. A. Cuomo *et al.*, The *Fusarium graminearum* genome reveals a link between localized polymorphism and pathogen specialization. *Science* **317**, 1400–1402 (2007).
25. Z. Hou *et al.*, A mitogen-activated protein kinase gene (*MGV1*) in *Fusarium graminearum* is required for female fertility, heterokaryon formation, and plant infection. *Mol. Plant-Microbe Interact.* **15**, 1119–1127 (2002).
26. K. S. Bruno, F. Tenjo, L. Li, J. E. Hamer, J. R. Xu, Cellular localization and role of kinase activity of *PMK1* in *Magnaporthe grisea*. *Eukaryotic Cell* **3**, 1525–1532 (2004).
27. X. Zhou, G. Li, J. R. Xu, Efficient approaches for generating GFP fusion and epitope-tagging constructs in filamentous fungi. *Methods Mol. Biol.* **722**, 199–212 (2011).

28. D. Chen *et al.*, Sexual specific functions of Tub1 beta-tubulins require stage-specific RNA processing and expression in *Fusarium graminearum*. *Environ. Microbiol.* **20**, 4009–4021 (2018).
29. C. Feng *et al.*, Uncovering Cis-regulatory elements important for A-to-I RNA editing in *Fusarium graminearum*. *mBio* **13**, e0187222 (2022).
30. Y. Liao, G. K. Smyth, W. Shi, featureCounts: An efficient general purpose program for assigning sequence reads to genomic features. *Bioinformatics* **30**, 923–930 (2014).
31. J. H. Yu *et al.*, Double-joint PCR: A PCR-based molecular tool for gene manipulations in filamentous fungi. *Fungal Genet. Biol.* **41**, 973–981 (2004).
32. C. Jiang *et al.*, An expanded subfamily of G-protein-coupled receptor genes in *Fusarium graminearum* required for wheat infection. *Nat. Microbiol.* **4**, 1582–1591 (2019).
33. J. M. Eggington, T. Greene, B. L. Bass, Predicting sites of *ADAR* editing in double-stranded RNA. *Nat. Commun.* **2**, 319 (2011).
34. M. R. Green, J. Sambrook, Polyacrylamide gel electrophoresis. *Cold Spring Harb. Protoc.* 525–532 (2020).
35. D. Kim, B. Langmead, S. L. Salzberg, HISAT: A fast spliced aligner with low memory requirements. *Nat. Methods.* **12**, 357–360 (2015).
36. D. W. Barnett, E. K. Garrison, A. R. Quinlan, M. P. Stromberg, G. T. Marth, BamTools: A C++ API and toolkit for analyzing and managing BAM files. *Bioinformatics* **27**, 1691–1692 (2011).
37. E. Picardi, G. Pesole, REDItools: High-throughput RNA editing detection made easy. *Bioinformatics* **29**, 1813–1814 (2013).
38. N. L. Catlett, B. N. Lee, O. C. Yoder, B. G. Turgeon, Split-marker recombination for efficient targeted deletion of fungal genes. *Fungal Genet. Rep.* **50**, 9–11 (2003).
39. C. Wang *et al.*, Functional analysis of the kinome of the wheat scab fungus *Fusarium graminearum*. *PLoS Pathog.* **7**, e1002460 (2011).
40. Z. Y. Bian, Z. Y. Wang, D. W. Wang, J. R. Xu, Fusarium graminearum raw sequencing reads PRJNA1031222. NCBI BioProject. https://www.ncbi.nlm.nih.gov/bioproject/PRJNA1031222. Deposited 23 October 2023.